General Disclaimer

One or more of the Following Statements may affect this Document

- This document has been reproduced from the best copy furnished by the organizational source. It is being released in the interest of making available as much information as possible.

- This document may contain data, which exceeds the sheet parameters. It was furnished in this condition by the organizational source and is the best copy available.

- This document may contain tone-on-tone or color graphs, charts and/or pictures, which have been reproduced in black and white.

- This document is paginated as submitted by the original source.

- Portions of this document are not fully legible due to the historical nature of some of the material. However, it is the best reproduction available from the original submission.

JOINT INSTITUTE FOR ADVANCEMENT OF FLIGHT SCIENCES

ACOUSTIC ANALYSIS OF THE PROPFAN

NASA GRANT NSG 1474

FINAL REPORT

(NASA-CR-162312) ACOUSTIC ANALYSIS OF THE PROPFAN Final Report (Joint Inst. for Advancement of Flight Sciences) 42 p
HC A03/MF A01 CSCL 21E G3/07

N79-32210
Unclas
35830

School of Engineering and Applied Science
The George Washington University
Washington, D. C. 20052

A REVIEW OF PROPELLER NOISE PREDICTION TECHNOLOGY WITH EMPHASIS ON TWO CURRENT METHODS FOR TIME DOMAIN CALCULATIONS

F. Farassat*

Joint Institute for Advancement of Flight Sciences
The George Washington University
Hampton, Virginia 23665

G. P. Succi**

Department of Aeronautics and Astronautics
Massachusetts Institute of Technology
Cambridge, Massachusetts

ABSTRACT

A review of propeller noise prediction technology is presented which highlights the developments in the field from the successful attempt of Gutin to the current sophisticated techniques. Two methods for the prediction of the noise from conventional and advanced propellers in forward flight are described. These methods developed at MIT and NASA Langley Research Center are based on different time domain formulations. Brief description of the computer algorithms based on these formulations are given. The output of these two programs which is the acoustic pressure signature, is Fourier analyzed to get the acoustic pressure spectrum. The main difference between the programs is that the Langley program can handle propellers with supersonic tip speed while the MIT program is for subsonic tip speed propellers. Comparisons of the calculated and measured acoustic data for a conventional and an advanced propeller show good agreement in general.

---

*Currently with the Acoustics and Noise Reduction Division, NASA-Langley Research Center, Mail Stop 461, Hampton, VA 23665.

**This work was partially completed when the author was Visiting Research Scientist at JIAFS.

INTRODUCTION

The technology for propeller noise prediction has been under development for many years. There is a new interest in accurate prediction methods for propeller noise because of the public pressure to reduce noise pollution and to meet government noise regulations. This paper presents two basically equivalent methods which were developed at Langley and at MIT respectively, and which have been used very successfully in predicting the noise of propellers. The success of these methods depends on the selection of appropriate acoustic formulations and the computer algorithms to implement these formulations. Before these methods are discussed in detail a short review of previous attempts to predict propeller noise will be presented.

REVIEW OF PREDICTION TECHNOLOGY DEVELOPMENT

A good review of aerodynamic sound of rotating blades was published by Morfey [1]. In the following, the emphasis will be on prediction techniques only. Propeller noise generation has a great deal of similarity to those of other members of rotating blade machinery such as fans and helicopter rotors. Often research findings on fans and rotors have resulted in a better understanding of propeller noise generation and thus improving its prediction.

The first successful prediction theory was by Gutin [2]. Gutin replaced the effect of blade forces on the fluid by a distribution of oscillating forces in the propeller disk. He then used a result of Lamb for the acoustic field of a stationary oscillating point force and the superposition principle, to calculate the level of the harmonics of the acoustic pressure. The success of this theory to calculate the first few

harmonics of propellers with low tip speed is well known. Only loading noise, that is the noise due to the forces on the fluid, was considered by Gutin.

Ernsthausen in Germany [3] and Deming in the U.S. [4] were among the first researchers to recognize the importance of noise generated by virtue of the finite blade thickness. Ernsthausen qualitatively explained the origin and characteristics of this noise. However, it was Deming who correctly formulated this problem theoretically. Each blade segment is assumed to generate a periodic disturbance in the propeller disk which can be Fourier analyzed into stationary but pulsating distributed sources along the path of the blade segment. Deming converted the problem of the determination of the sound generated by a non-lifting blade into the equivalent problem of the sound from a continuous distribution of piston sources radiating into a half-space. Using the superposition principle he obtained an expression for the far-field thickness noise. Because of the limited computing capability of the 1930's, Deming had to make some simplifying assumptions in his acoustic calculations. He obtained generally good agreement with experimental data upto the highest test tip Mach number of about 0.7.

Another significant step in the prediction of the noise of propellers was taken by Garrick and Watkins [5]. They extended the work of Gutin to propellers in forward flight. The acoustic sources were again distributed on the entire propeller disk. Each source on the disk travels retilinearly. A simple geometrical construction was used to obtain the source position

at the emission time and the relative position of the source and the observer used in acoustic calculations. This geometrical construction is sometimes called the Garrick triangle. Garrick and Watkins considered loading noise in their analysis although their method could be used to extend Deming's thickness noise analysis to propellers in forward flight.

In the mid-fifties, Arnoldi obtained an expression for thickness noise in the frequency domain [6]. His result was developed for compact blade sources in contrast to Deming's analysis which was for noncompact sources. Arnoldi's expression is relatively simple and is comparable to Gutin's result for the loading noise.

In the early sixties, Van de Vooren and Zandbergen obtained a solution for the acoustic field of a singularity in helical motion [7]. They applied this solution to calculate the thickness and loading noise of propellers in forward flight. Although their numerical results are for a single singularity, in principle their method can be used for a surface distribution of sources by dividing the blades into panels and using the superposition principle. Unfortunately the above method, which requires a computer for acoustic calculations, did not receive proper attention.

Since the early sixties, considerable research has been done on the understanding of the noise mechanisms and the prediction of the noise of rotating blades. The development of high speed digital computers helped the researchers to use more realistic models in their study. Some of the more recent developments in mathematics, such as generalized function theory, simplified the process of finding the solution of the wave

equation of acoustics with moving volume and surface sources. One successful attempt was the solution obtained by Lowson for a moving point source [8]. His simple, but powerful, result for a point force in motion, incorporates much of the earlier results which were obtained by classical mathematics. Using more sophisticated mathematics Ffowcs Williams and Hawkings published a paper in which they derived the now famous Ffowcs Williams-Hawkings (FW-H) equation [9]. The acoustic analogy was applied to obtain a wave equation for the fluid density in the medium around a body in arbitrary motion. Although reference to turbulence is made in the title of this paper, the current applications of the theory of these authors are limited to surface sources. One significant contribution of Ffowcs Williams and Hawkings was to write their solution of the acoustic wave equation (FW-H EQ.) in various forms. In a particular problem, some of these forms are more appropriate than others. It is less known that a paper published by Möhring, Müller and Obermeier at about the same time that the paper by Ffowcs Williams and Hawkings appeared, is closely related to the latter authors' work [10].

When acoustic sources are in motion, the apparent extent of the source to an observer who receives the sound can change considerably. If the source motion, its frequency of fluctuations and the observer position are such that the source can be treated as a moving point source, it is said to be compact. Otherwise it is noncompact. Ffowcs Williams and Hawkings formalized the treatment of the acoustics of noncompact sources. The prediction methods discussed here are for noncompact sources.

Upto the late sixties, it was believed that the thickness noise of rotating blades was not significant enough to be included in acoustic calculations. This belief, based partly on qualitative reasoning, could

not be justified because of the evidence to the contrary in the published literature. The works of Arnoldi [6] and Van de Vooren and Zandbergen [7] indicated that thickness and loading noise components can be of comparable magnitude for typical operating conditions of a propeller. More recently, it was Lyon who found out by a numerical method that the thickness noise can be the dominant noise component in the plane of a helicopter rotor at high blade tip speeds [11]. This conclusion, of course, applies directly to the propeller noise problem. Since the publication of this paper, many other workers in this field have derived various equivalent formulations of thickness noise [12-17]. These formulations can all be related to the various forms of the solution of the FW-H equation.

One discovery that has important bearing on the work presented here was that static propellers generated more noise than propellers in forward flight. Similar behavior has also been observed for the fan of turbofan engines. It was Hanson's idea that the discrepancy, which was observed at high harmonics of the measured sound, was due to differences in fluctuating load levels in the cases of static fans and those in forward flight [18]. In the case of static fans, the turbulent eddies are stretched to considerable length while being sucked into the fan, and thus cause fluctuating forces on the blades. Fans in flight fly into the turbulent eddies thus giving them much less time to stretch out and to cause fluctuating blade loading. This idea of Hanson has been verified by experiments that used instrumented blades. A similar study on propellers by Hamilton Standard for NASA established that the same phenomenon is also at work in propellers [19,20]. The importance of fluctuating blade loading on noise generated by helicopter rotors has also been known for many

years. In the case of propellers, noise measured in the regions where the surface sources appear compact, is influenced greatly by fluctuating blade loading. For conventional static propellers, high harmonics of measured sound are primarily due to fluctuations in blade loading even where steady blade loading and thickness sources are noncompact. A compact source calculation for fluctuating blade loading together with a noncompact source calculation for thickness and steady loading noise appears to be the best approach for predicting the noise of static propellers [20].

The latest development in this field has been the realization of the importance of nonlinearities in the flow-field around the blades [21, 22]. Some nonlinear effects can be inferred when linear acoustic calculations are compared with measured propeller noise data. For instance, the calculated width of the acoustic pressure signature is narrower than the measured width. For conventional propellers this difference does not appear to be significant. However, one phenomenon, when not taken into consideration in linear acoustic calculations, can lead one to suspect erroneously the importance of nonlinear effects. This phenomenon is the interaction of propeller blades with the flow-field established around the aircraft nacelles, wings and fuselage. The blades sense a periodic load, once per revolution, due to asymmetry in the airflow into the propeller. This blade load variation increases the levels of the low harmonics of the acoustic pressure spectrum. In the examples presented in this paper for a general aviation propeller these blade load variations are included in calculations and they have noticeable effect on the results.

As discussed above, there have been considerable gains in knowledge and experience on propeller noise. It is now possible to calculate

propeller noise with good accuracy. This paper presents two related methods with different capabilities. In studying the acoustic of rotating blades it becomes obvious that a closed form analytic solution always requires some unwanted restrictions such as far-field positioning of the observer. The frequency domain approach restricts the observer to move with the propeller. To have the least restrictive prediction method, a time domain numerical approach seems the best choice and the methods reported here work in the time domain.

In the next section, the analytic formulations are derived. Brief descriptions of algorithms used in the computer codes are then presented. The inputs to these programs are blade geometry, loading and the propeller motion. The acoustic pressure signature and spectrum are the outputs. These programs are identified as the MIT and the Langley programs.

To demonstrate the applications of these programs, several examples related to a series of flight tests on a three bladed propeller will be presented. One of the blades was instrumented with pressure gauges which responded to the fluctuations in surface pressure. It was found that each blade experienced a large fluctuating load with fundamental frequency equal to the shaft frequency. This fluctuation was caused by nonuniform flow into the propeller due to the presence of the wing and engine intake blockage. Both steady and fluctuating loads were included in the calculations. The agreement of theoretical and measured data is generally good. The MIT program was used for these calculations.

Some calculated acoustic pressure signatures and spectra of a propeller with advanced blade geometry (prop-fan) operating at supersonic tip

speeds are presented. These were computed by means of the Langley program. In general the agreement with the experimental data is good. Some nonlinear effects are observed which are discussed in the paper.

THEORETICAL FORMULATIONS

In this section the formulations used in the noise prediction programs will be presented. The starting point of the analysis is FW-H equation without the quadrupole term [9]:

$$\frac{1}{c^2}\frac{\partial^2 p'}{\partial t^2} - \nabla^2 p' = \frac{\partial}{\partial t}\left[\rho_0 v_n |\nabla f| \delta(f)\right] - \frac{\partial}{\partial x_i}\left[l_i |\nabla f| \delta(f)\right] \tag{1}$$

where p' is the acoustic pressure, ρ_0 and c are the density and speed of sound in the undisturbed medium respectively, v_n is the local normal velocity on the surface of a given body $f(\vec{x},t)=0$ in motion. The local force on the fluid (per unit area) at the surface of the body is denoted by l_i and $\delta(f)$ stands for the Dirac delta function.

The solution of Eq. (1) of interest here has been published elsewhere [13,23]. The derivation will not be repeated here. The solution can be written in terms of two integrals over the surface.
Σ: $f(\underset{\sim}{y};\underset{\sim}{x},t) = f(\underset{\sim}{y},t-r/c) = [f(\underset{\sim}{y},\tau)]_{ret} = 0$, where $r = |\underset{\sim}{x}-\underset{\sim}{y}|$. It is

$$4\pi p'(\underset{\sim}{x},t) = \frac{1}{c}\frac{\partial}{\partial t}\int_{f=0}\frac{1}{r}\left[\frac{\rho_0 c\, v_n + l_r}{\Lambda}\right]_{ret} d\Sigma + \int_{f=0}\frac{1}{r^2}\left[\frac{l_r}{\Lambda}\right]_{ret} d\Sigma \tag{2}$$

where $l_r = l_i \hat{r}_i$ and $\hat{r}_i = (x_i - y_i)/r$ is the unit vector in the radiation direction. If dS is the element of the surface area of the body $f=0$ and $d\Gamma$ is an element of the length of the curve of intersection of this body and the sphere $g=\tau-t+r/c=0$, then it can be shown that

$$\frac{d\Sigma}{\Lambda} = \frac{dS}{|1-M_r|} \tag{3-a}$$

$$= \frac{c\ d\Gamma\ d\tau}{\sin\theta} \tag{3-b}$$

here $M_r = v_i \hat{r}_i / c$, v_i is the local velocity of the body surface and θ is the angle between the outward normal to the body surface and $\hat{r}_i$. The source time is denoted τ. Using Eq. (3) in Eq. (2), the following two equations are obtained.

$$4\pi p'(\underset{\sim}{x},t) = \frac{1}{} \frac{\partial}{\partial t} \int_{f=0} \left[\frac{\rho_0 c\ v_n + l_r}{r|1-M_r|}\right] dS + \int_{f=0} \left[\frac{l_r}{r^2|1-M_r|}\right]_{ret} dS \tag{4-a}$$

$$= \frac{\partial}{\partial t} \int_{\substack{f=0 \\ g=0}} \frac{\rho_0 c\ v_n + l_r}{r\ \sin\theta}\ d\Gamma\ d\tau + \int_{\substack{f=0 \\ g=0}} \frac{c l_r}{r^2 \sin\theta}\ d\Gamma\ d\tau \tag{4-b}$$

Depending on the value of M_r, one of the two expressions in Eq. (4) is used in acoustic calculations. In the program available at Langley, these equations are used without further modifications.

It is common practice to break down the acoustic pressure into components. Thickness, loading and skin friction noise are contributions of the terms in Eq. (4) involving v_n, the surface pressure p in l_i and the tangential stress due to skin friction in l_i, respectively.

Another form of acoustic equations is to represent the radiation field as the sum of the acoustic pressure from an array of point sources. Each point source is characterized by a volume ψ and force L_i. The points are located by slicing the blades into many small segments. Each segment has an associated volume, a force due to surface pressure and tangential

force due to skin friction. Together, these yield a point volume source and a point force source for each blade segment. The derivation of these equations from FW-H equation was developed in [17].

The acoustic pressure $p'(x,t)$ is written as

$$p'(x,t) = \sum_k (p'_{fk} + p'_{vk}) \tag{5}$$

where p'_{fk} is the acoustic pressure due to point force by kth segment producing loading and skin friction noise and p'_{vk} is the acoustic pressure due to a volume source by that segment (producing thickness noise). These two terms are given by

$$4\pi p'_{fk} = \{\frac{1}{r}\frac{1}{|1-M_r|^2}[\frac{\hat{r}_i}{c}\frac{\partial L_i}{\partial \tau} + \frac{\hat{r}_i}{|1-M_r|}(\frac{\hat{r}_i}{c}\frac{\partial M_i}{\partial \tau})] + \frac{1}{r^2}\frac{1}{|1-M_r|^2}[r_j L_j \frac{1-M_i^2}{|1-M_r|} - L_i M_i]\}_{ret} \tag{6-a}$$

$$4\pi p'_{vk} = \rho_0 \frac{\partial^2}{\partial t^2}[\frac{\psi_k}{r|1-M_r|}]_{ret}$$

$$= \rho_0 \{\frac{1}{|1-M_r|}\frac{\partial}{\partial \tau}[\frac{1}{1-M_r}\frac{\partial}{\partial \tau}(\frac{\psi_k}{r|1-M_r|})]\}_{ret} \tag{6-b}$$

where ψ_k is the volume of the kth blade segment. Equation (6-a) is identical to Lowson's result for a point force in motion originally published in [8] and used extensively by him for helicopter rotor noise calculation. The derivation of the thickness noise formulation used in Eq. (6-b) can

be found in references [17,23]. For numerical calculatio , the source time differentiations are carried out explicitly. As in the case of Lowson's result, the acceleration of the volume source, described by the term $\partial M_r/\partial \tau$ has considerable influence on the radiated sound.

COMPUTATIONAL METHODS

In this section a brief review of computational methods used in the two programs will be presented. The input information for both programs is identical. The following groups of input data are required:

1. Geometric Data:

   a. Blade radius and planform; blade chord, thickness ratio, and twist distributions as a function of radial position.

   b. Airfoil section description as a function of radial position.

   c. Observer mode of motion, stationary or moving with the propeller.

2. Aerodynamic Data: Blade surface pressure and skin friction coefficient distribution.

3. Operating Data: Propeller RPM and forward speed.

The programs differ in details and capabilities. The MIT program is for general aviation propellers having subsonic tip speed. It can handle blades with in-plane sweep. Its chief advantage is simplicity and speed of computation. The Langley program can handle supersonic blade tip speeds and the noise of advanced propellers with out-of-plane blade sweep, such as the prop-fan designed by Hamilton Standard, can be calculated. It is more complex and takes longer to execute on a computer. Some more details of these two programs follow.

The MIT Program

The MIT Program is divided into three sections: the blade description, the blade pressure signature, and the Fourier analysis. The blade is described in the input file by a polynomial expansion of its shape and by similar expansions of the in-plane and out-of-plane loading. In addition, information is included as to the mesh size for segmenting the blade.

The mesh size is varied in both the chordwise and spanwise directions so as to allow the user some flexibility in performing the calculations. For example, a rough calculation can be made with only one point per blade for design purposes, or, the mesh size can be graded coarsely on the inboard stations and finely on the outboard station so as to provide an efficient computation scheme for analyzing experimental data. Ultimately, the MIT Program replaces the blade with an array of spiraling point sources, each with a unique force vector and volume. To do this the blade mid-chord is described first and the blade span is divided into strips by cuts perpendicular to radii drawn to specified stations on the centerline. These strips are further divided in the chordwise direction. The blade segments are thus constructed. The volume and force on the fluid by each blade segment are assigned to points at the center of these segments.

The second part of the program deals with the calculation of the blade pressure signature. The observer location at time t is specified; currently the options are for a stationary observer or for one moving with the forward velocity of the propeller. For this time t, there is

an associated emission time τ for each blade segment which is calculated by an iterative scheme. Given the retarded time, the contribution of a particular segment is evaluated exactly according to Eq. (6). A summation over all blade segments yields the pressure signature at observer time t. Numerical integration or differentiation is not needed in this scheme. The only numerical work is involved in calculating the emission time.

The above procedure is repeated for other observer times to obtain the acoustic pressure signature. Given the pressure signature the program then computes the Fourier analysis. The spectra are also A weighted so as to provide useful output for designers. The flow chart for this program is presented in Fig. 1.

The Langley Program

In the Langley program, the propeller blade is described by first specifying the leading edge curve in the Cartesian coordinate system fixed to the blade. In general this is a three-dimensional curve when the airfoil shape and the geometric angle of attack are given in planes normal to the pitch change axis as shown in Fig. 2. A curvilinear coordinate system (Q,η_2) describes the surface of each blade. Here Q is the nondimensional distance from the leading edge (based on local chord) in a plane normal to the pitch change axis. The radial distance of this plane from the axis of rotation is η_2. The blade is subdivided by specifying ΔQ and $\Delta\eta_2$. In general the blade panels look like parallelograms rather than rectangles. Near the leading edge of the blade smaller chordwise division are selected. Also smaller spanwise divisions near the blade tip are needed due to the higher helical speed.

For thickness noise, the upper and lower surface panels are both used in the summation approximating the relevant integrals in Eq. (4). For loading and skin friction noise, only the panel on the plane of the chord was used. This was found to be appropriate since in aerodynamic calculations, often only the local lift distribution is calculated. If $\underset{\sim}{\eta}(Q,\eta_2)$ is the position vector for points on the surface of a blade, then the surface area of a panel is given by

$$\Delta S = \left|\frac{\partial \underset{\sim}{\eta}}{\partial Q} \times \frac{\partial \underset{\sim}{\eta}}{\partial \eta_2}\right| \Delta Q \Delta \eta_2 \tag{7}$$

The local unit normal used in the calculation of the normal velocity is found from:

$$\underset{\sim}{n} = \left(\frac{\partial \underset{\sim}{\eta}}{\partial Q} \times \frac{\partial \underset{\sim}{\eta}}{\partial \eta_2}\right) \Big/ \left|\frac{\partial \underset{\sim}{\eta}}{\partial Q} \times \frac{\partial \underset{\sim}{\eta}}{\partial \eta_2}\right| \tag{8}$$

To calculate the emission time two schemes are used. For panels with subsonic helical speeds a scheme which adjusts the source time τ to make $g=\tau-t+r/c$ approach zero is used. This scheme is very fast. For panels with transonic or supersonic helical speed, the method of regula falsi [24] is used to solve for the emission times. It was found unnecessary to calculate the emission times for upper and lower surface panels separately. The emission times of the center points of the panels on the camber surface were used for panels which lie on the actual blade surface directly above and below these panels. The two methods of finding emission times will be called scheme 1 and 2, respectively in the flow-chart for this program.

For panels with $M_r<1$, Eq. (4-a) is used in discrete form. Equation (4-b) in discrete form is used for panels with $M_r=1$ or $M_r>1$. In this case, the collapsing sphere method is used for each panel individually. To obtain good accuracy, at least ten intersections of the collapsing sphere and the panel are used for approximating the integrals in Eq. (4-b). Figure 3 shows the flow chart for the Langley program.

The Langley program is more complex and is slower than the MIT program. Comparison of the outputs of MIT and Langley programs with identical inputs, have convinced the authors that the results of the two programs are virtually identical for propellers with subsonic helical tip speeds.

Both the Langley and the MIT programs can handle cases where the observer is in motion with the propeller. This is achieved by noting that if $\underset{\sim}{x}_m$ is the position of the observer in the moving frame, then the observer position in the frame fixed to the undisturbed medium is

$$\underset{\sim}{x}_f = \underset{\sim}{x}_m + \int_0^t \underset{\sim}{v}(t')\, dt' \tag{9}$$

where $\underset{\sim}{v}(t')$ is the forward velocity of the propeller. Therefore in the moving frame $p'(\underset{\sim}{x}_m,t)=p'(\underset{\sim}{x}_f,t)$. Note that $\underset{\sim}{x}_f=\underset{\sim}{x}_f(\underset{\sim}{x}_m,t)$ and this is known if the motion of the propeller is specified.

COMPARISON WITH EXPERIMENTAL DATA

In this section theoretical calculations of propeller noise will be compared with measured acoustic data for a conventional propeller and an advanced propeller.

A General Aviation Propeller

This set of measurements is well documented [19]. A twin-engine, high wing, light STOL transport was used with two microphones on the portside wing tip, one in the propeller plane at 7.28m from the axis of rotation. The second microphone was at the same distance from the propeller axis but 3.05m behind the propeller plane. The flight tests were conducted with the starboard engine shut down. The propeller had three blades with a diameter of 2.59m and its RPM (100%) was 2200. The blade form curves are shown in Fig. 4. One blade was instrumented with seven pressure transducers which responded to local surface pressure variation on the pressure side of the blade.

For comparison, five tests were selected from the published test report [19]. To reduce confusion, the same run number designations are used in this paper as in that report. Table 1 summarizes the operating conditions for the test runs. The acoustic pressure spectra for the two microphones for all test runs are available in [19]. Some acoustic pressure signatures were produced from recorded test data for this paper. The MIT program was used to obtain the theoretical acoustic pressure signatures and spectra.

The aerodynamic calculations are based on a modification of Goldstein's theory by Larabee [25]. The net thrust and torque in Table 1 are calculated by this method for which the propeller is assumed to be operating at minimum induced loss. To the authors' knowledge, there are no reliable in-flight aerodynamic data for propellers to substantiate this assumption. However, the calculated radial distribution of the blade loads for five runs, Fig. 5 appear reasonable.

In the aerodynamic theory of propellers one assumes that the lift vector is not perpendicular to the kinematic velocity of the blade section. The perturbation to the flow field by the propeller must be included in calculating the velocity field; hence the lift is perpendicular to the total velocity which is the vector sum of the kinematic velocity plus the induced velocity. Given the lift vector, the surface friction effect are included in the standard manner by assuming they are perpendicular to the lift vector and equal in magnitude to (C_D/C_L) times the lift force. The drag-to-lift ratio used in the calculations was the optimum (C_D/C_L) for the series 16 airfoil used on this propeller.

An approximation was made in that the chordwise distribution of the friction forces was assumed to be identical to the lift forces. This approximation is not critical as the calculation of the pressure signature is much more sensitive to the radial load distribution. The chordwise blade description is much more important in calculating the thickness noise. This noise is sensitive to chordwise variations of the volume distribution at tip speeds greater than Mach 0.75. The contribution of the friction forces to the overall noise of the propeller was so small that it could be neglected in acoustic calculations. This is in agreement with the findings of Farassat et al [26]. However, in the results reported here, it was added to the loading noise and not calculated separately.

The test result showed that due to flow asymmetry, the unsteady part of the surface pressure varied in phase for all transducer positions almost sinusoidally. The flow asymmetry was caused by engine blockage

and the frequency of the variation was the same as the shaft frequency. The positive peak appeared when the blade was in the third quadrant of the propeller disk when viewed from front. The amplitude of this pressure variation was large enough to produce large variation in blade load. It was estimated that the amplitude of the first harmonic blade load varied upto 20 percent of the steady load. Higher harmonics of the load variation were negligible. For this reason, in the following calculations, this unsteady loading component is included. Note that in all the theoretical results, the observer is in motion with the propeller.

Figure 6 shows the influence of the chordwise loading and the unsteady loading discussed above on the calculated noise for run 8. It is seen that for uniform loading, the inclusion of unsteady loading has increased the level of all the calculated harmonics only very slightly. Using a more realistic chordwise distribution which peaks at the blade leading edge (of the form a Ax^4 where A=constant and x is the distance from T.E.), there is further increase in the level of high harmonics of the calculated noise. This fact was pointed out by Hanson [27] but has been known for some time. Figures 7 and 8 show the calculated and measured acoustic pressure signatures and spectra for runs 2 and 3A. The agreement of the calculated and measured results is very good. The signatures for loading and thickness noise of run 2 are presented in Fig. 9. One can see that both thickness and loading noise are of the same order of magnitude and neither can be neglected in calculations. In all theoretical calculations, a chordwise loading with the peak at the leading edge has been used.

It is well-known that the blade tip speed strongly influences the noise of propellers. This can be seen in Fig. 10 where the two acoustic pressure spectra presented correspond to helical tip speeds 190.9m/sec and 230.1m/sec. In the latter case, the acoustic spectrum falls off less rapidly and the overall noise level is considerably higher than that of the lower tip speed case.

On the whole, it can be said that the in-flight propeller noise of general aviation aircraft can be predicted with reliable precision. One should have some knowledge of aerodynamic blade load variation due to either the influence of flow around the aircraft or the propeller plane angle with free stream velocity vector. Apart from loading noise, thickness noise must be included in calculations but the skin friction noise is negligible.

An Advanced Propeller

The Langley program was used to calculate the noise of prop-fan designed by Hamilton Standard. Acoustic test data for a 2-bladed model prop-fan (SR-1 Model) with swept blade were supplied by the manufacturer. The data were collected in UTRC open jet anechoic tunnel. The jet Mach number was 0.32 (106.3m/sec). The blade radius was 0.31m and the helical tip speed of the model was 343.7m/sec (M=1.03). The blade form curves and a sketch of the untwisted planform are presented in Fig. 11. This design was not acoustically optimized and was used to study the effectiveness of blade sweep in reducing the radiated noise. The calculated radial distribution of blade lift coefficient is presented in Fig. 12. The net torque, thrust and power of the model were 37N-m, 325N and 39KW respectively. The microphones were outside the tunnel jet shear layer.

Figures 13 and 14 present the calculated and measured acoustic pressure signatures and spectra for two microphone positions. The microphone positions and the level of the measured noise harmonics have been corrected for the tunnel jet shear layer effect using Amiet's theory. The microphone positions shown in the figures, which were used in theoretical calculations, correspond to positions where the microphones would be if the jet diameter was large enough to enclose them. These corrections were supplied by the manufacturers also. The moving microphone option of the acoustic program was therefore used for these calculations. The chordwise loading was assumed to be parabolic. This assumption was probably not realistic. There are little theoretical or experimental aerodynamic data on thin airfoils in the range of Mach numbers encountered in the test. Therefore, this assumption must be considered one source of error. These two figures present typical results of many similar calculations.

From these figures, it is seen that the theoretical pressure signatures closely resemble the measured signatures. The theoretical and measured acoustic spectra also show reasonably good agreement with some exceptions. The level of the low harmonics of the acoustic spectrum is underestimated by about 5 dB in Fig. 13. This discrepancy is more pronounced where thickness noise is the dominant component of the noise. It is now generally believed that this is a nonlinear flow effect. Yu et al [21] and Hanson and Fink [22] have attempted to account for this discrepancy by including in their acoustic calculations the quadrupole source term appearing in FW-H Eq. This approach requires almost as much effort as needed to solve the flow problem around the blades which would make the acoustic calculations redundant.

Another point of disagreement between the measured and calculated acoustic spectra is that the first dip in the experimental spectrum appears at a lower frequency than that of the calculated spectrum. This is related to the width of the main pulse in the acoustic pressure signature which is larger in the measured than the calculated signature. This disagreement is also believed to be due to flow nonlinearities which is neglected in acoustic calculations. This weakness of linear acoustic theory to account properly for the width of the main pulse of the pressure signature was pointed out by Boxwell, Schmitz and Yu [27].

Although linear acoustic theory has some shortcomings, it can be a very useful tool in the design stage of propellers. It is believed that the noise regulations for propeller-driven aircraft will be based on taxiing or flight conditions. The methods presented here will be suitable for estimation of the noise of these aircraft.

CONCLUDING REMARKS

This paper discusses two methods for the calculation of propeller noise. The formulations used in these methods and a brief discussion of Algorithms employed in two computer programs developed at MIT and at Langley are presented. The programs differ in capability and complexity. The main difference between the two programs is that the MIT program can only handle propellers with subsonic tip speed but the Langley program can also treat propellers with supersonic tip speed. All the acoustic calculations are performed in time domain. In subsonic cases, no noticeable difference between the outputs of the two programs were observed.

The noise of conventional propellers in forward flight can be predicted with good accuracy using only thickness and loading noise. Non-compact source formulation which accounts for differences in emission time for sources on the blade surface must be used. Low harmonics of blade loading due to flow asymmetry into the propeller must be included. The examples in this paper have shown that the thickness noise is an important component of the overall noise of conventional propellers. The noise due to tangential skin friction stress is negligible. It must be remembered that in general aviation aircraft there are other sources of sound than propellers such as the engine, which may influence the measured noise spectra considerably. These sources have not been discussed here.

For propellers with high tip speeds, linear acoustic theory which is used in the two programs discussed here, does provide good estimate of the radiated noise. There are two features of the measured acoustic pressures signature and spectrum that the linear theory does not account for. First, the calculated width of the main pulse of the pressure signature is narrower and the second is that the levels of the first few harmonics of the acoustic pressure spectrum are in many cases underestimated. Both these two features, which are believed to be due to nonlinearities in the flow around the blades, are prominant where the thickness noise component is significant. The deviation between measured and calculated results appear at transonic and supersonic tip speeds. Nevertheless, many acoustic calculations for propellers with advanced and conventional blade design have convinced the authors that the methods

presented here, when the results are properly interpreted with good engineering judgement, provide useful tools in estimating propeller noise in flight.

ACKNOWLEDGEMENTS

The works of G. P. Succi and F. Farassat were supported by NASA Contract No. NASI-15154 and NASA Research Grant No. NSG 1474, respectively. F. Farassat would like to thank Mr. P. A. Nystrom of the Acoustics and Noise Reduction Division of NASA Langley Research Center for his technical support. The help of the staff of the acoustics group of Hamilton Standard, particularly Mr. F. B. Metzger and Dr. D. B. Hanson for supplying technical data on prop-fan are gratefully acknowledged.

REFERENCES

1. C. L. Morfey 1973, 587-617. Journal of Sound and Vibration 28 (3) Rotating blades and aerodynamic sound.

2. L. Gutin 1936, Zhurnal Technicheskoi Fiziki 6, 899-909. (In Russian) Translated as 1948 NACA TM 1195: On the sound field of a rotating airscrew.

3. W. Ernsthausen 1936, Luftfahrtforschung 8 (12), 433-440. (In German)Translated as 1937 NACA TM 825: The source of propeller noise.

4. A. F. Deming 1938, NACA TN 679. Noise from propellers with symmetrical sections at zero blade angle, II.

5. I. E. Garrick and C. E. Watkins 1954 NACA Report 1198. A theoretical study of the effect of forward speed on the free-space sound-pressure field around propellers.

6. R. A. Arnoldi 1956 United Aircraft Corporation Research Department, East Hartford, Connecticut, Report R-0896-1. Propeller noise caused by blade thickness.

7. A. I. Van de Vooren and P. J. Zandbergen 1963, AIAA Journal 1, 1518-1526. Noise field of a rotating propeller in forward flight.

8. M. V. Lowson 1965 Proceedings of the Royal Society (London) A286, 559-572. The sound field for singularities in motion.

9. J. E. Ffowcs Williams and D. I. Hawkings 1969 Philosophical Transactions of the Royal Society (London) A264, 321-342. Sound generated by turbulence and surfaces in arbitrary motion.

10. W. F. Möhring, E. A. Müller and F. F. Obermeier 1969 Acoustica 21, 184-188. Schallerzeugung durch instationare stromung als singulare storungs problem.

11. R. H. Lyon 1971 Journal of Acoustical Society of America 49, 849-905. Radiation of sound by airfoils that accelerate near the speed of sound.

12. D. L. Hawkings and M. V. Lowson 1974 Journal of Sound and Vibration 36, 1-20. Theory of open supersonic rotor noise.

13. F. Farassat L975 NASA Technical Report R-451. Theory of noise generation from moving bodies with an application to helicopter rotors.

14. D. B. Hanson 1976 AIAA Paper 76-565. Near field noise of tip speed propellers in forward flight.

15. Y. Nakamura and A. Azuma 1978 NASA Conference Publication 2052, 323-337. Improved method for calculating the thickness noise.

16. C. J. Woan and G. M. Gregorek 1978 AIAA Paper 78-1122. The exact numerical calculation of propeller noise.

17. G. P. Succi 1979 SAE Paper 790584. Design of quiet efficient propellers.

18. D. B. Hanson 1975 AIAA Paper 75-468. Study of subsonic fan noise sources.

19. D. Magliozzi 1977 NASA Contractor Report 145105. The influence of forward flight on propeller noise.

20. R. J. Pegg, B. Magliozzi, and F. Farassat 1977 ASME Paper 77-GT-70. Some measured and calculated effects of forward velocity on propeller noise.

21. Y. H. Yu, F. X. Caradonna and F. H. Schmitz 1978 Paper No. 58, Fourth European Rotor Craft and Powered Lift Aircraft Forum, Stresa, Italy. The influence of the transonic flow field on high-speed helicopter impulsive noise.

22. D. B. Hanson and M. R. Fink 1978 paper presented at Spring Meeting of the Institute of Acoustics, Cambridge University, England. The importance of quadrupole sources in prediction of transonic tip speed propeller noise. (Also appeared in Journal of Sound and Vibration, 62, (1979) 19-38).

23. F. Farassat 1977 Journal of Sound and Vibration 55, 165-193. Discontinuities in aerodynamics and aeroacoustics: The concept and applications of generalized derivatives.

24. S. D. Conte and C. DeBoor 1972 Elementary Numerical Analysis, 2nd Edition, McGraw-Hill Book Company.

25. E. Larabee 1979 SAE Paper 790585. Practical design of minimum induced loos propellers.

26. F. Farassat, C. E. K. Morris and P. A. Nystrom 1979 AIAA Paper 79-0608. A comparison of linear acoustic theory with experimental noise data for a small scale hovering rotor.

27. D. A. Boxwell, Y. H. Yu and F. H. Schmitz 1978 NASA CP 2052, 309-322. Hovering impulsive noise - some measured and calculated results.

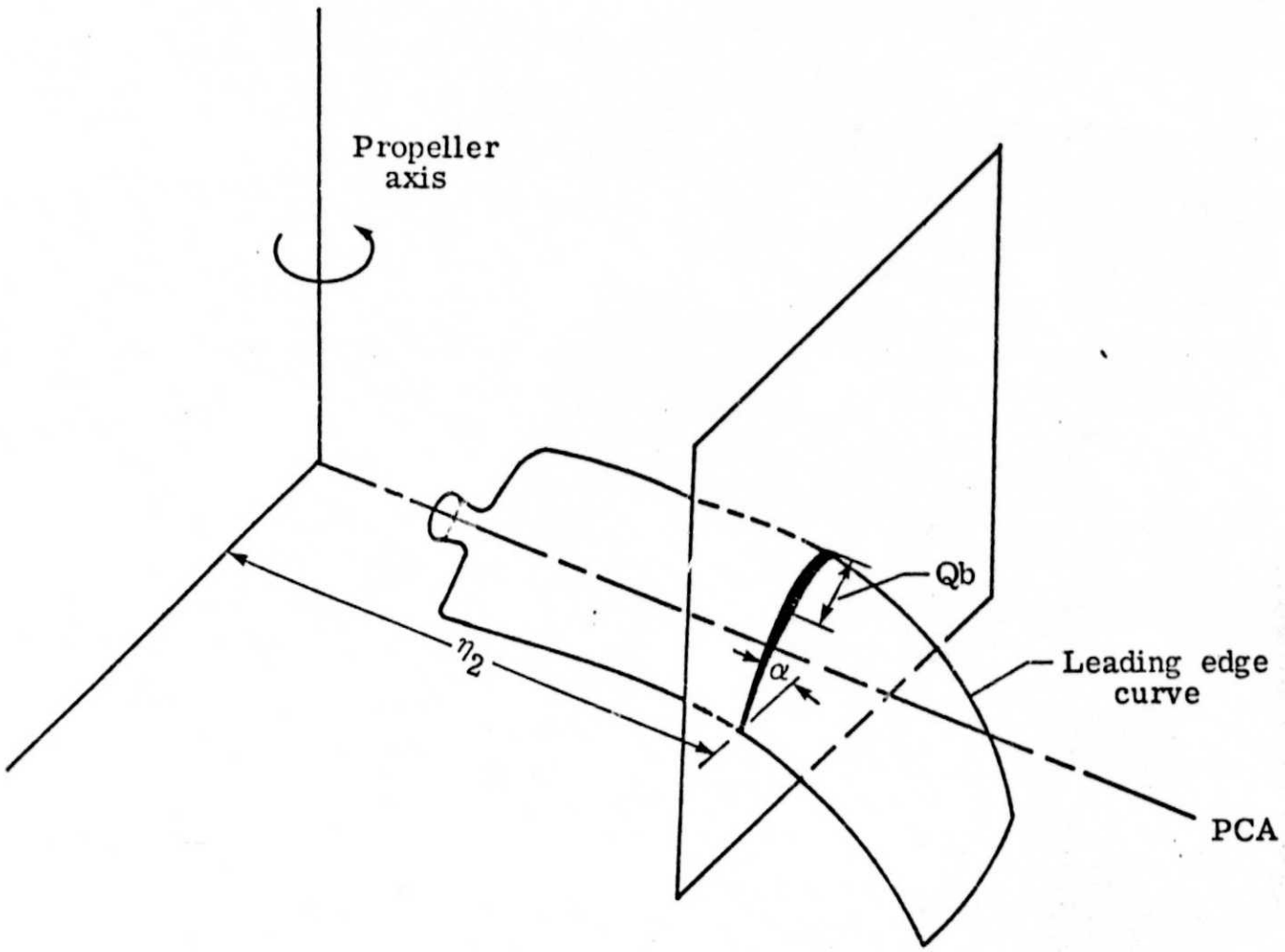

α = Geometric angle of attack (function of η_2)

PCA = pitch change axis

b = chord (function of η_2)

Q = distance from L.E./b

Figure 2. - Curvilinear Coordinate System (Q,η_2) used in the Langley Program to describe blade geometry of advanced propellers. The blade mean surface is not in a plane.

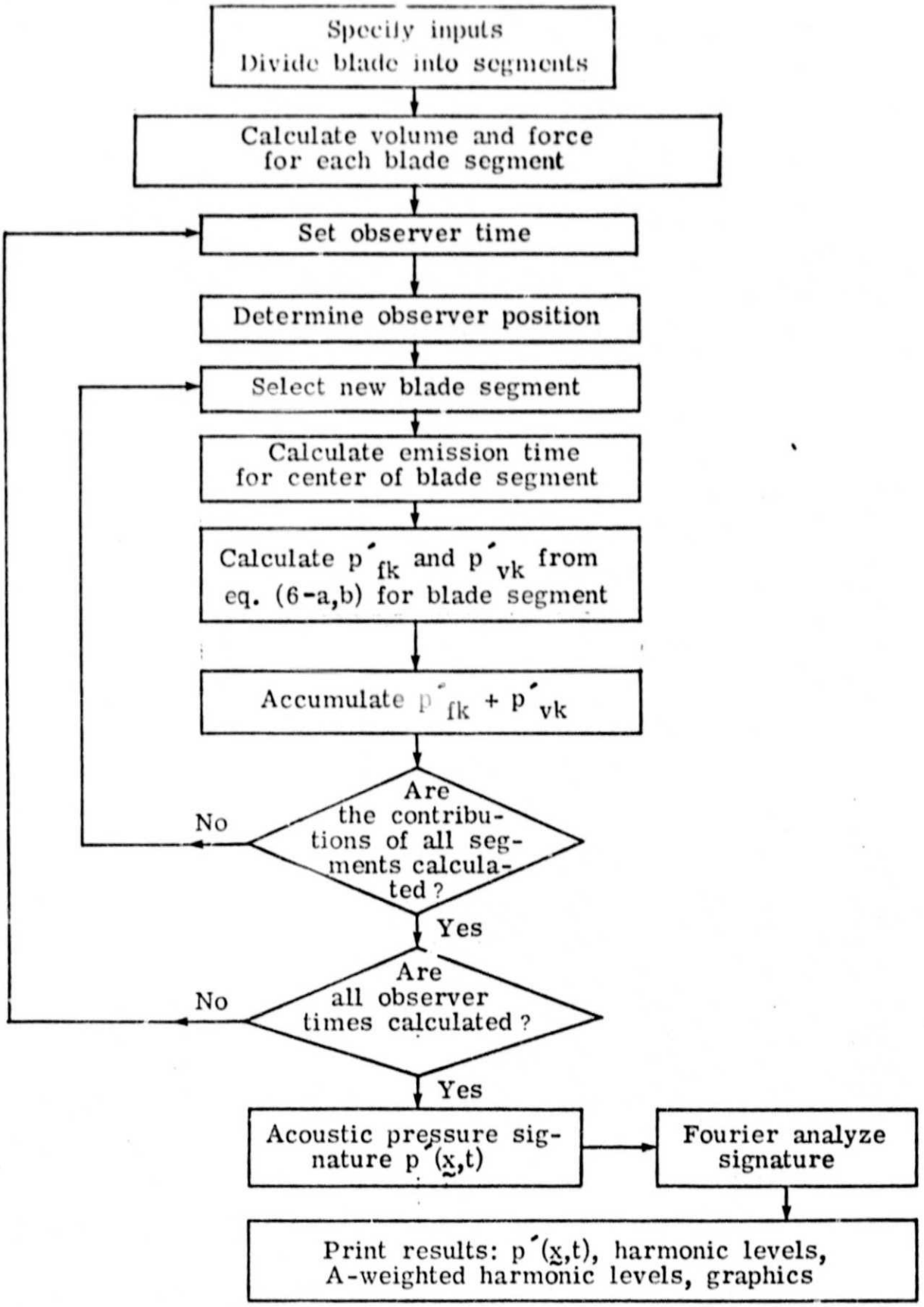

Figure 3. - Flow chart for Langley Acoustic Program.

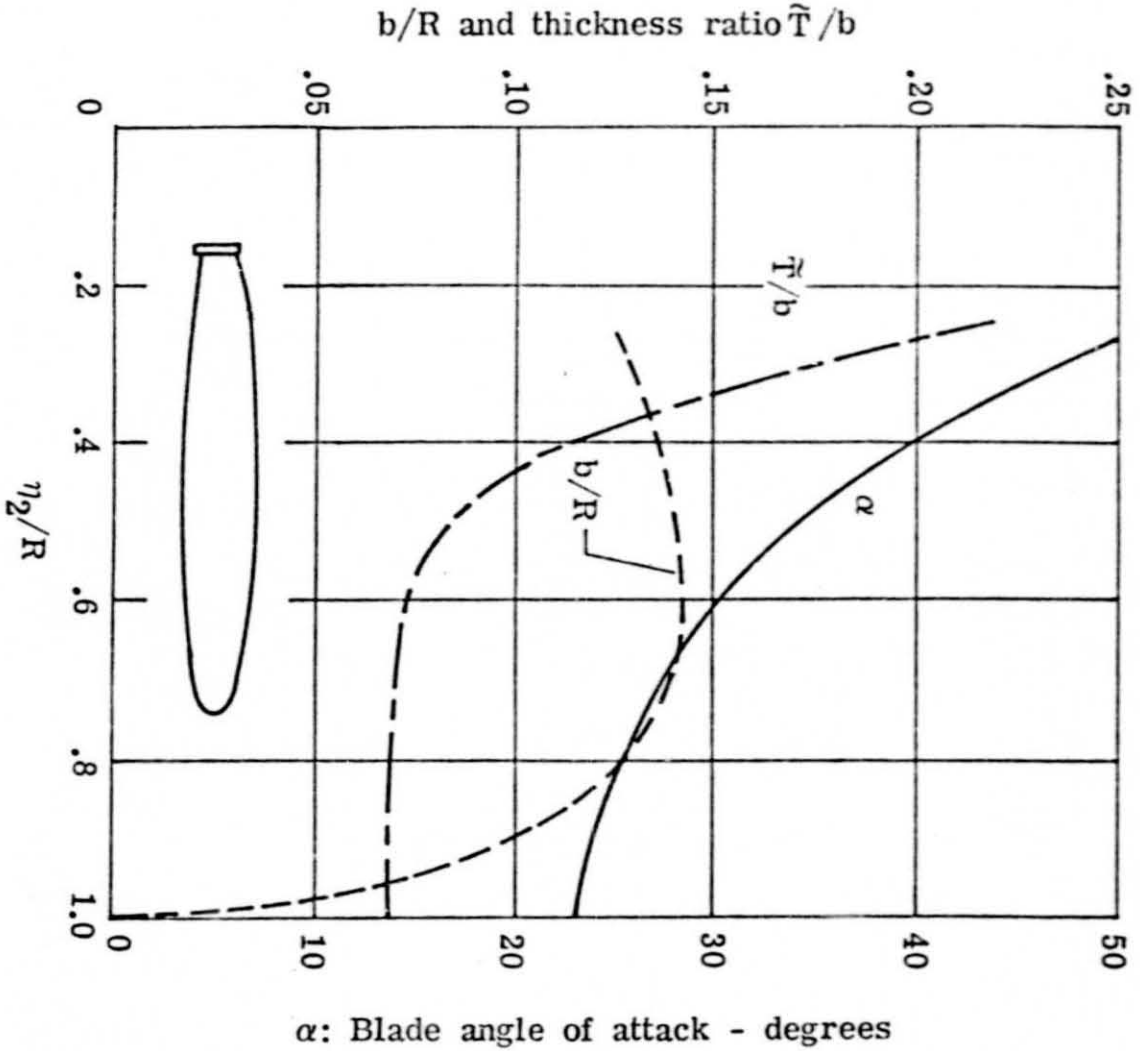

Figure 4. - Blade form curves and the planform for the general aviation propeller used for in-flight acoustic measurement. b = Chord, $\tilde{T}$ = maximum thickness of airfoil, R = blade radius, η_2 = distance from propeller center.

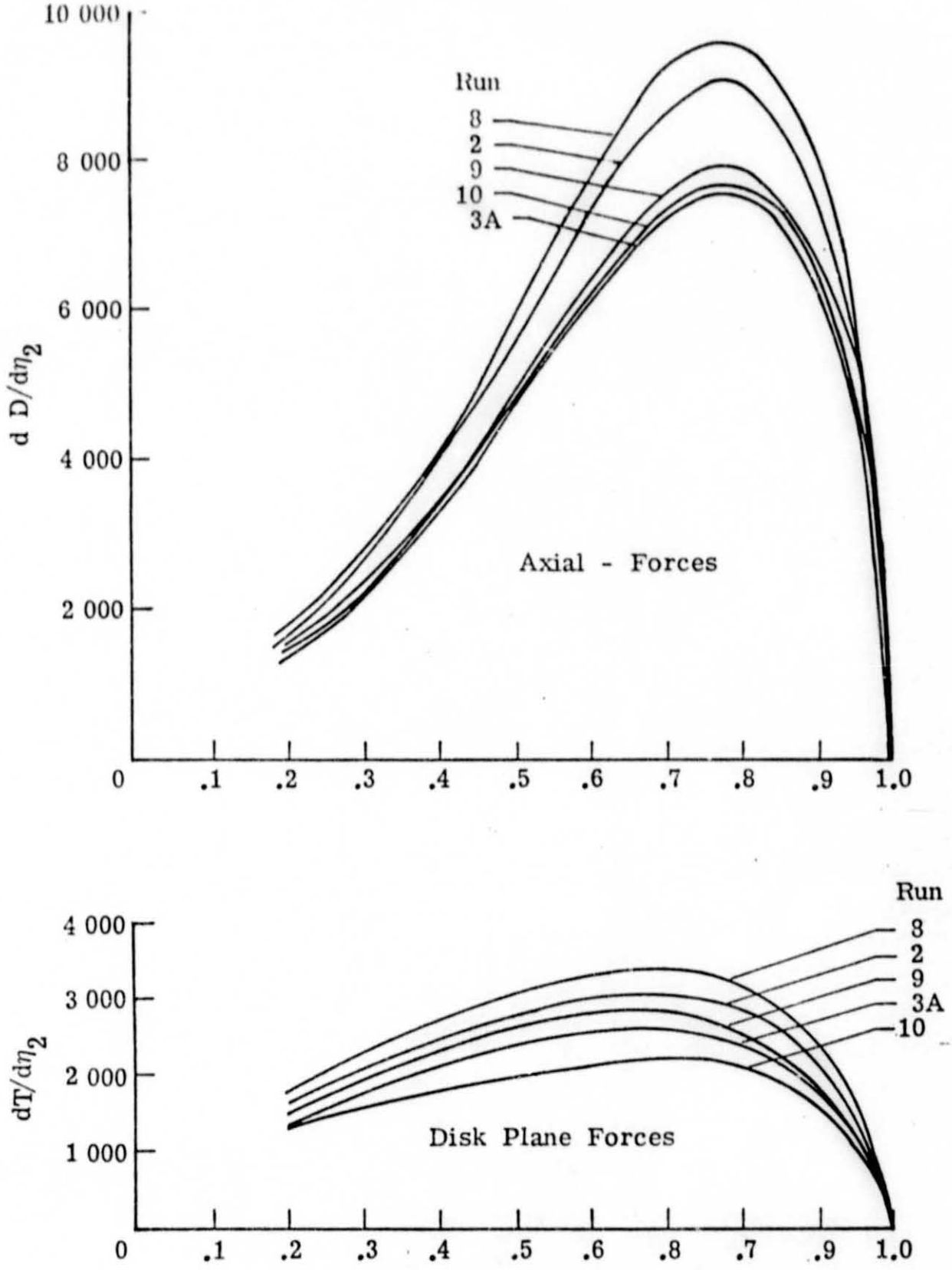

Figure 5. - Calculated variation of blade loads as a function of distance from propeller center η_2 for the five tests of the general aviation propeller. D = drag, T = thrust, R = blade radius.

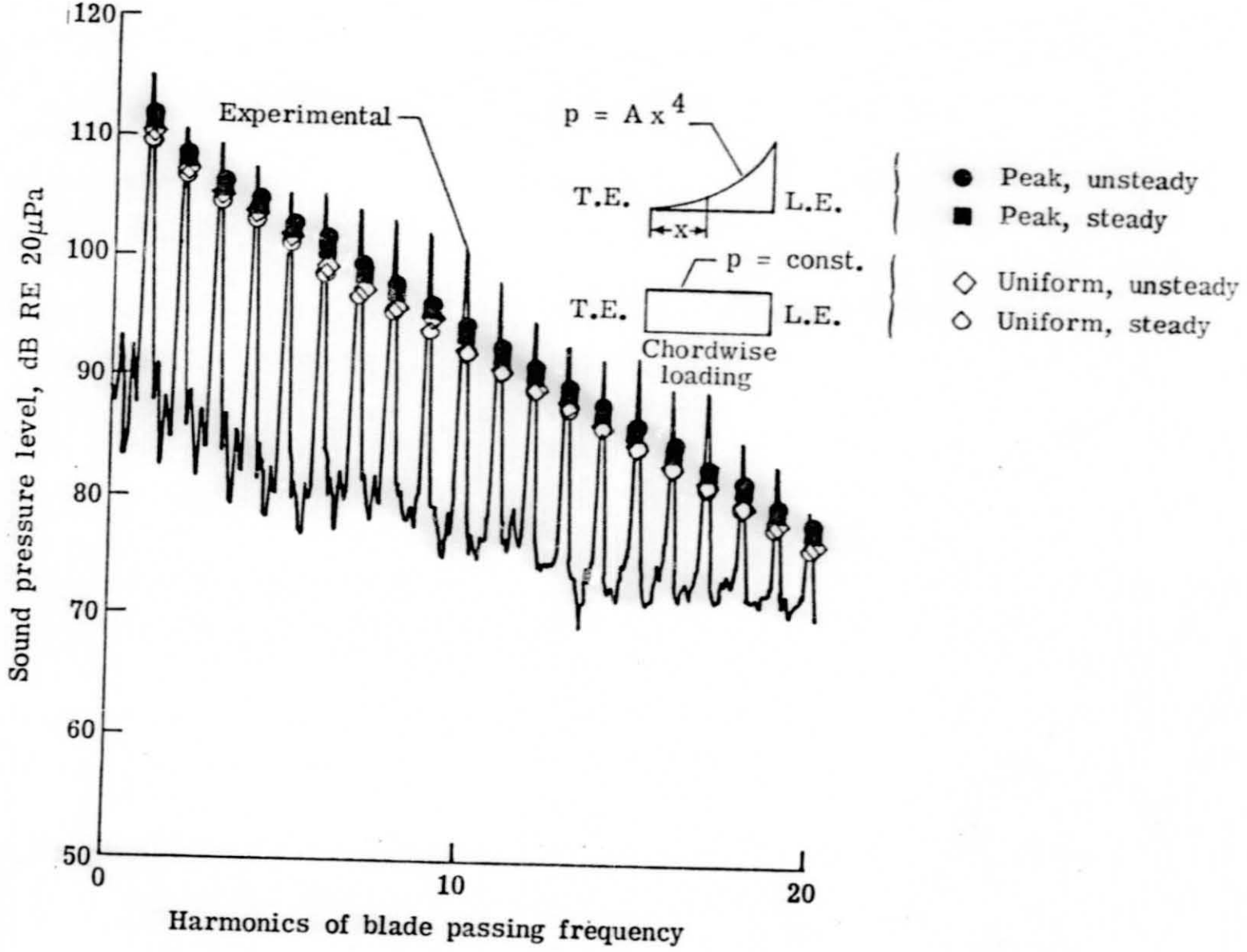

Figure 6. - The effect of chordwise loading and unsteady blade load variation on the calculated acoustic pressure spectrum and comparison with measured spectrum for Run 8. In-plane microphone

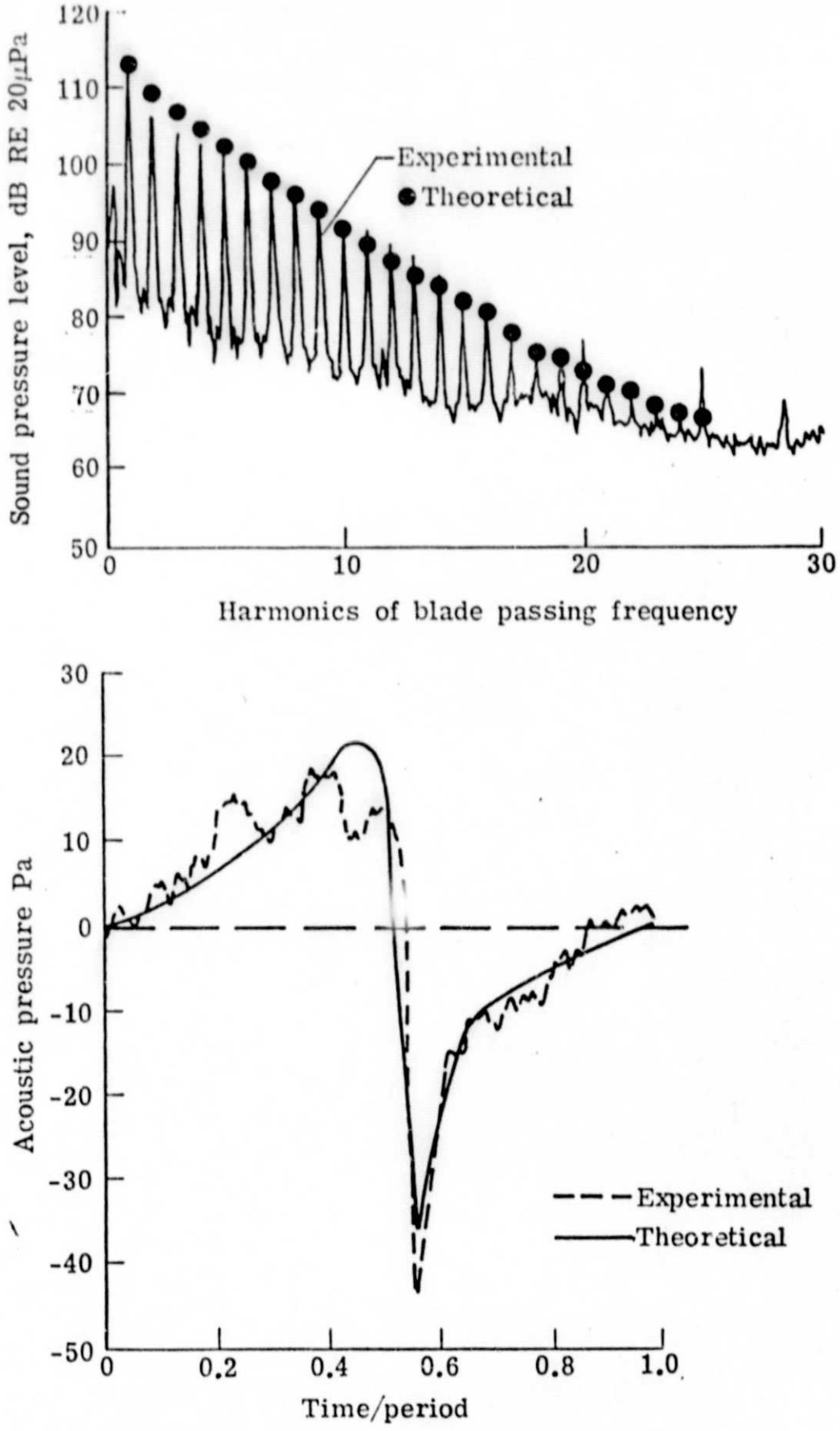

Figure 7(a). - Calculated and measured acoustic pressure signatures and spectra for the general aviation propeller. Run 2, In-plane microphone, Period = 9.32 msec

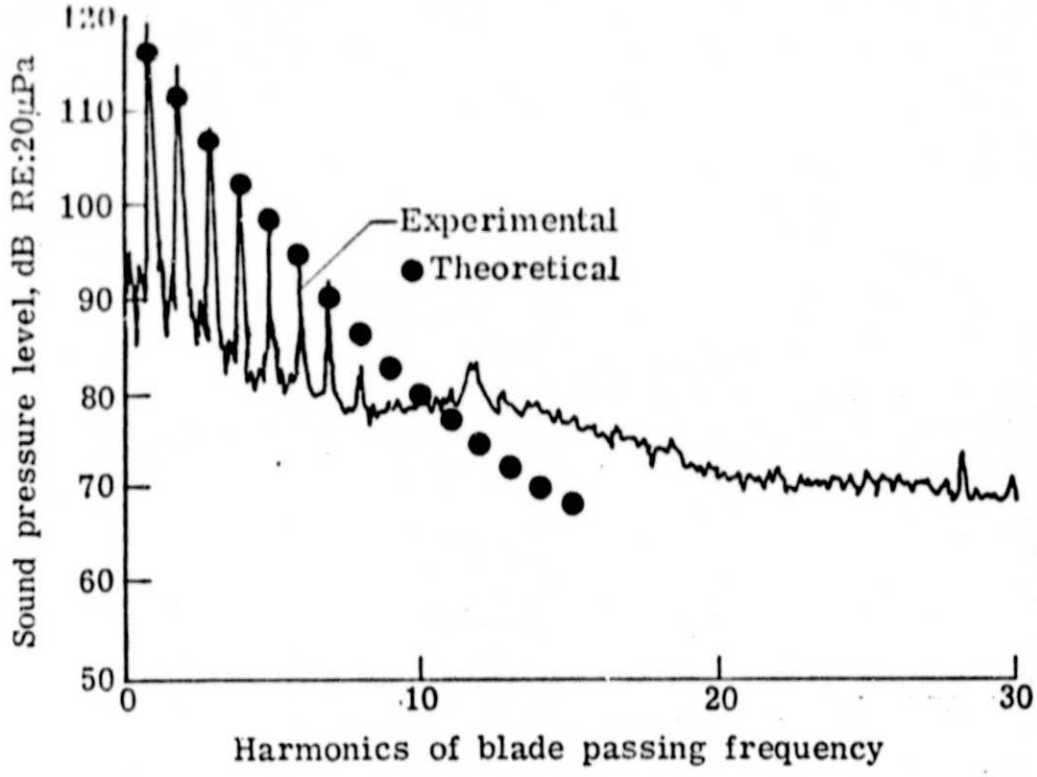

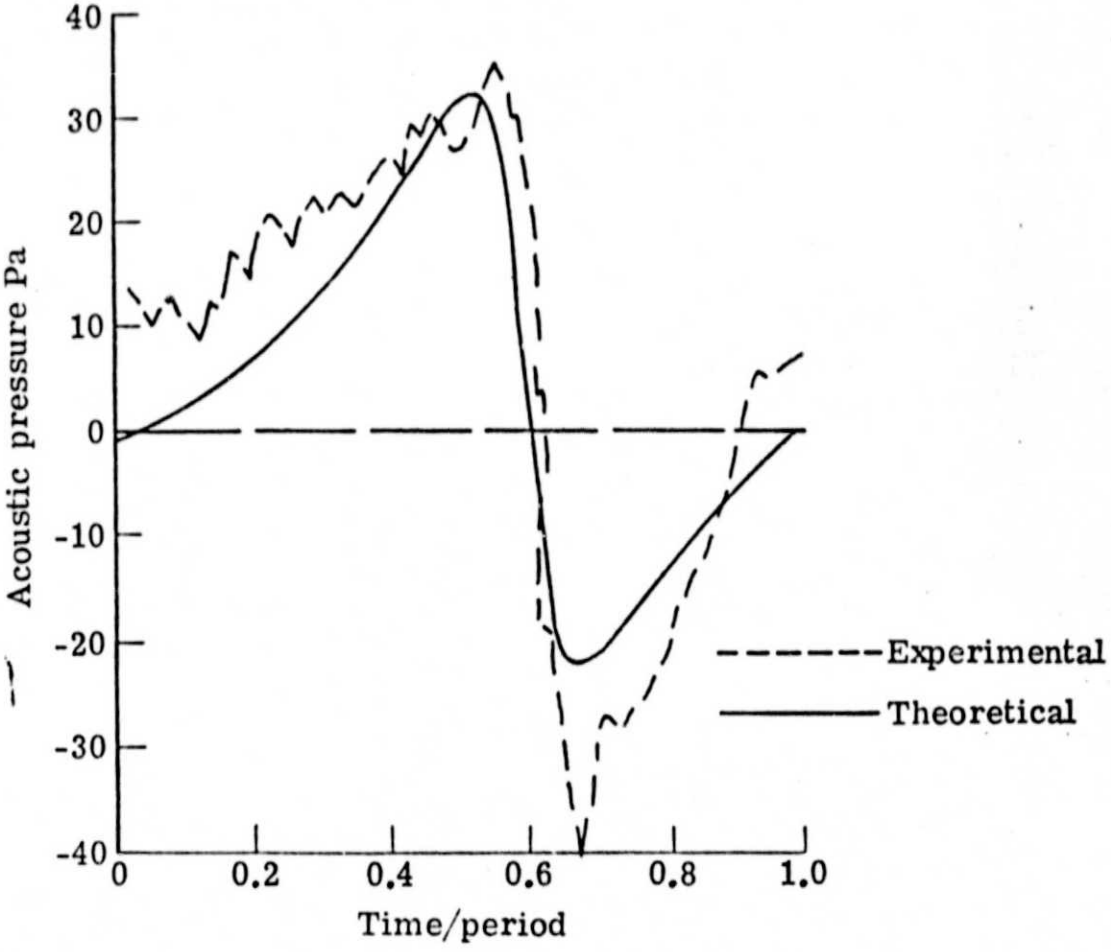

Figure 7(b). - Aft Microphone

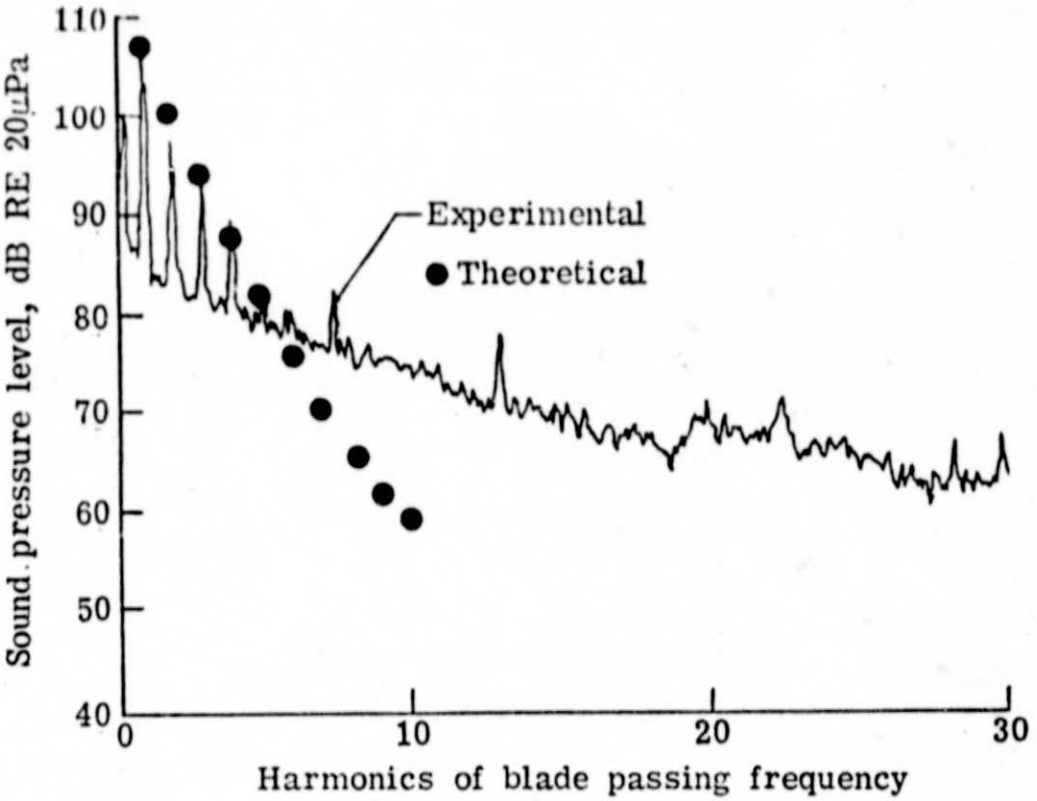

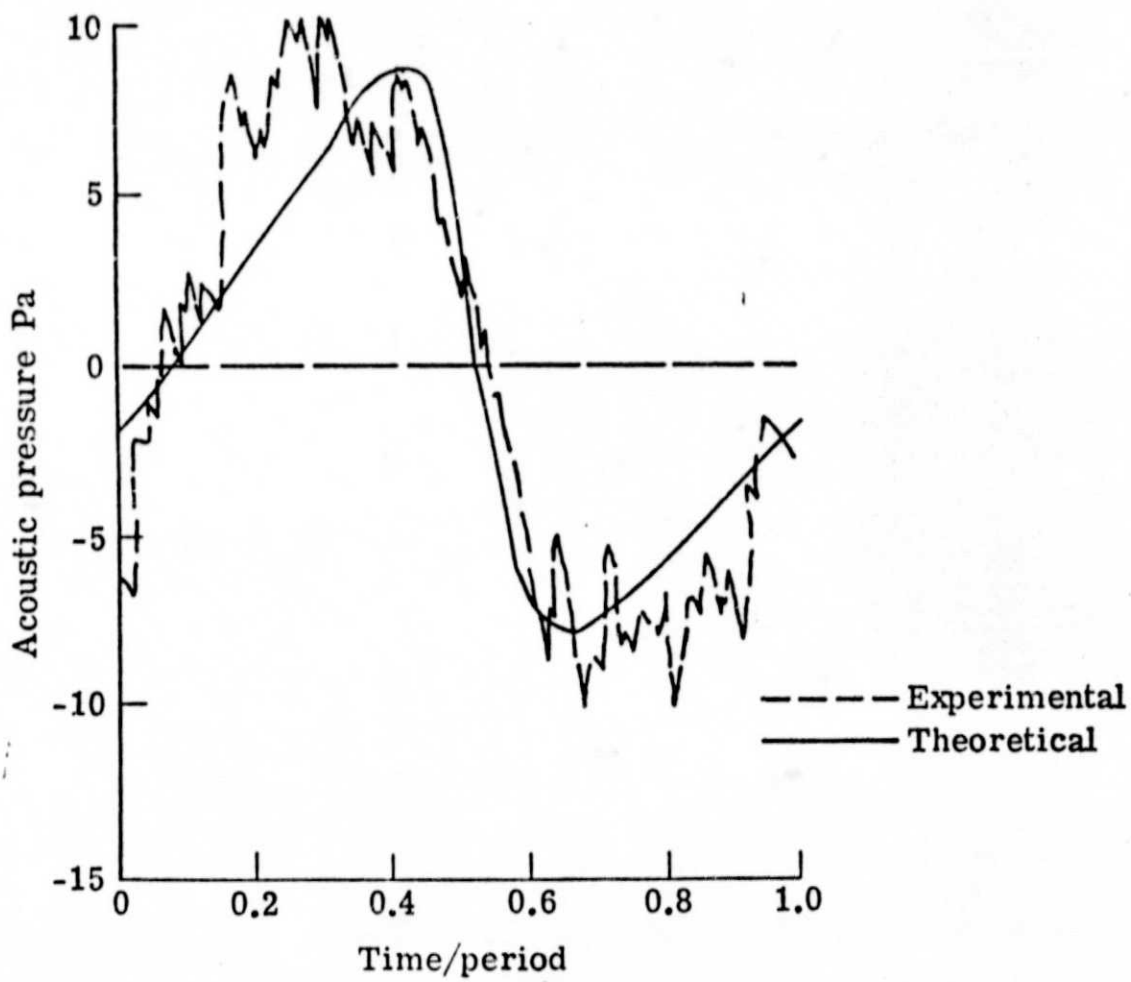

Figure 8(a).- Calculated and measured acoustic pressure signatures and spectra for the general aviation propeller. Run 3A, In-plane microphone, period = 11.36 msec.

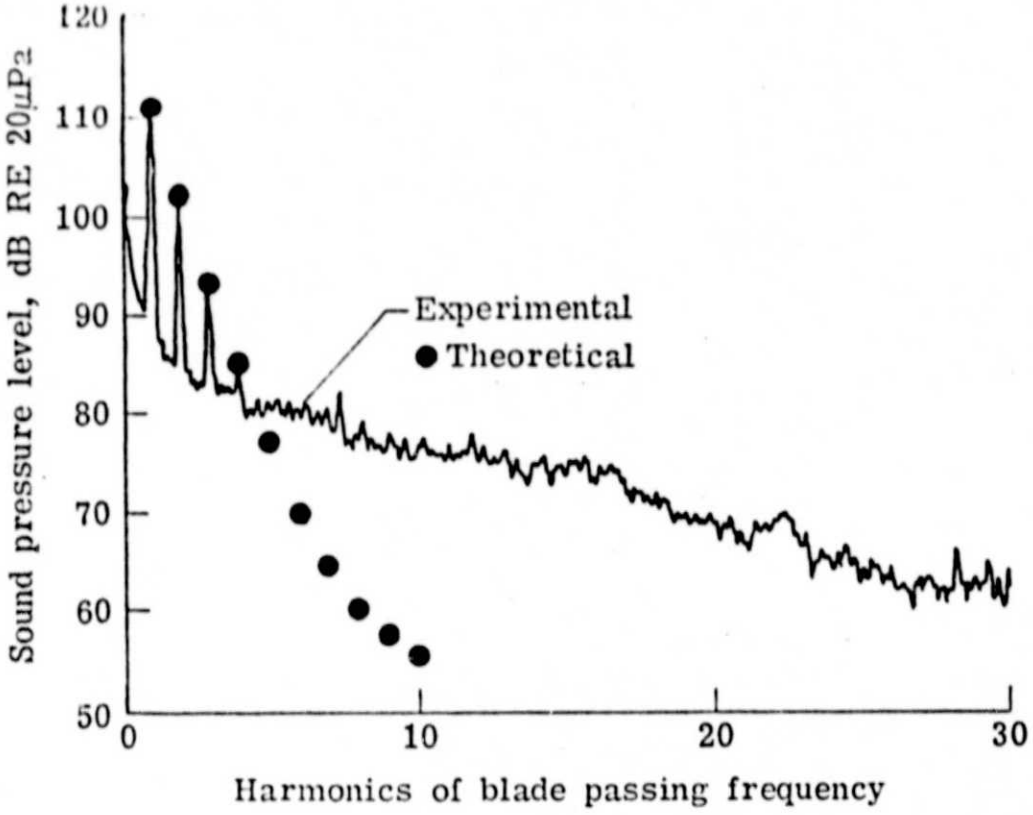

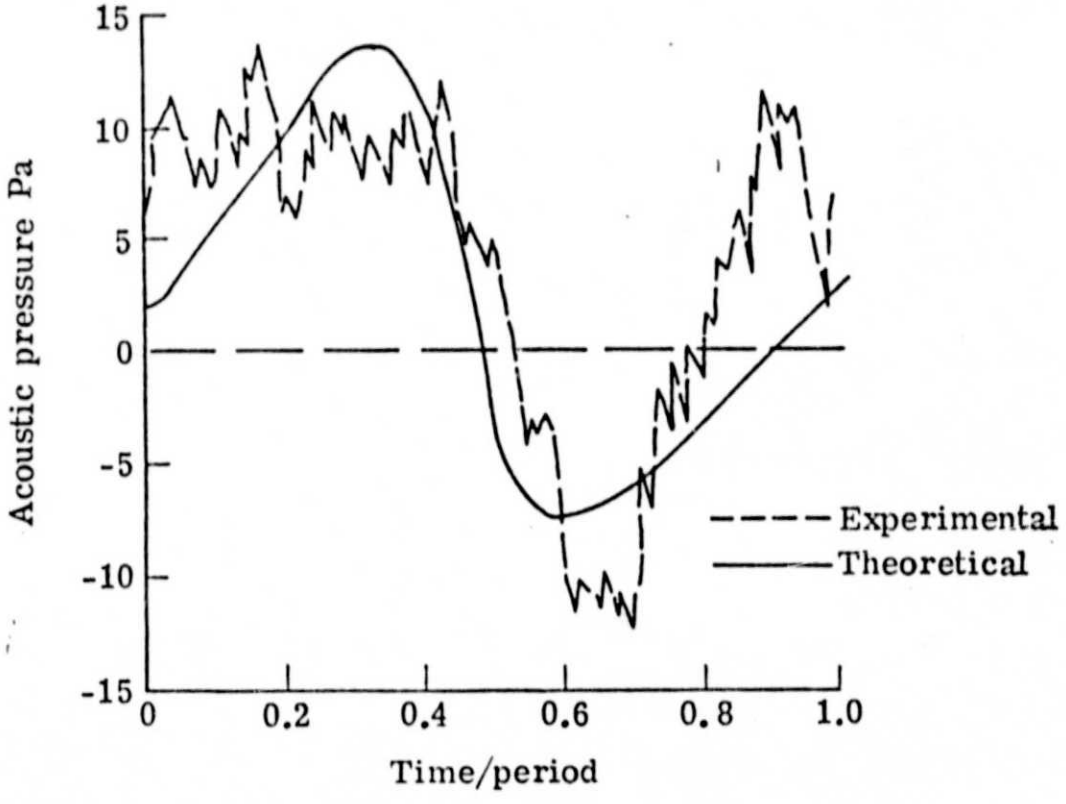

Figure 8(b).- Aft microphone.

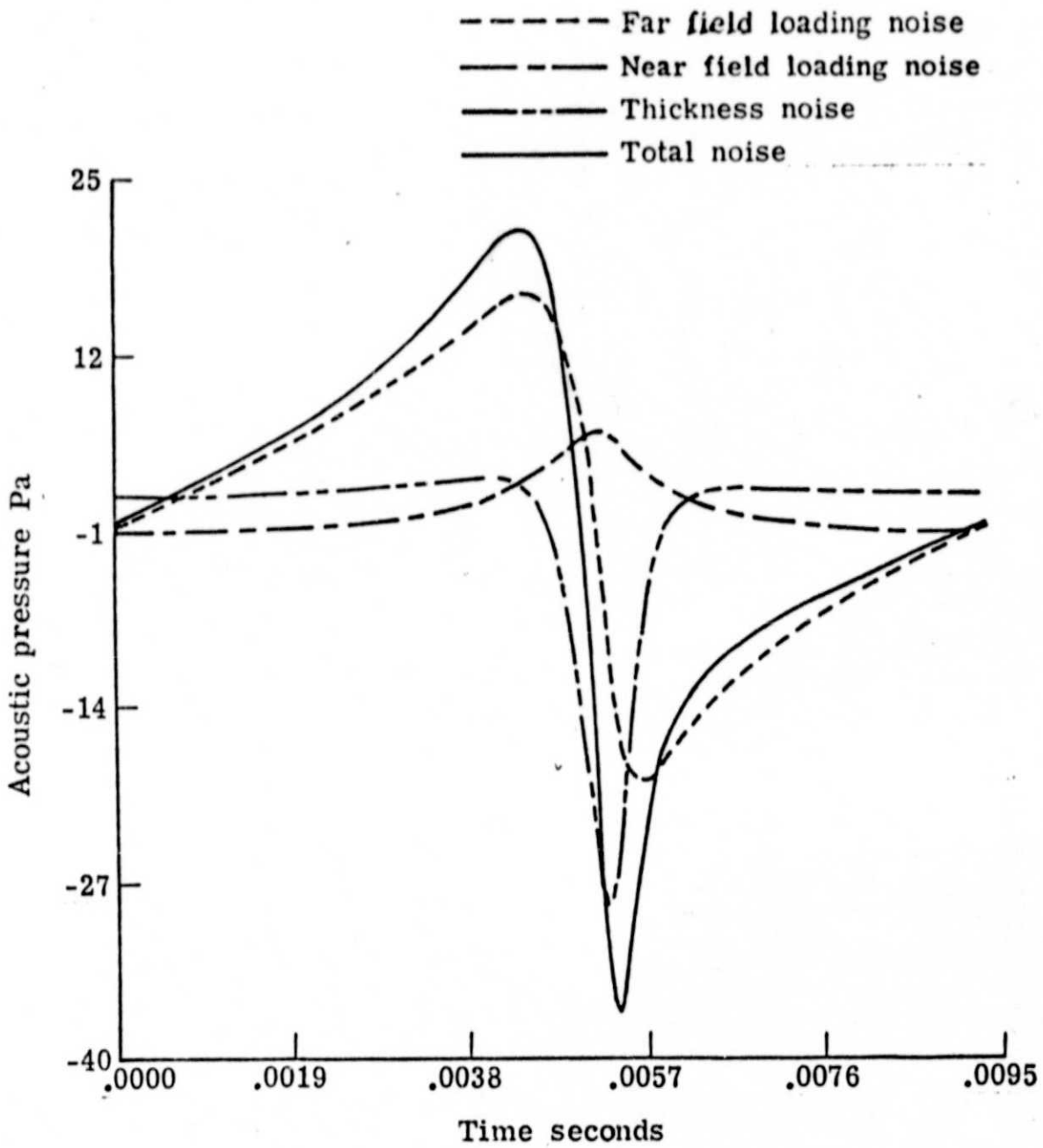

Figure 9.- Relative magnitudes of loading and thickness noise for in-plane microphone position, run 2. The effect of skin friction is included in the loading noise.

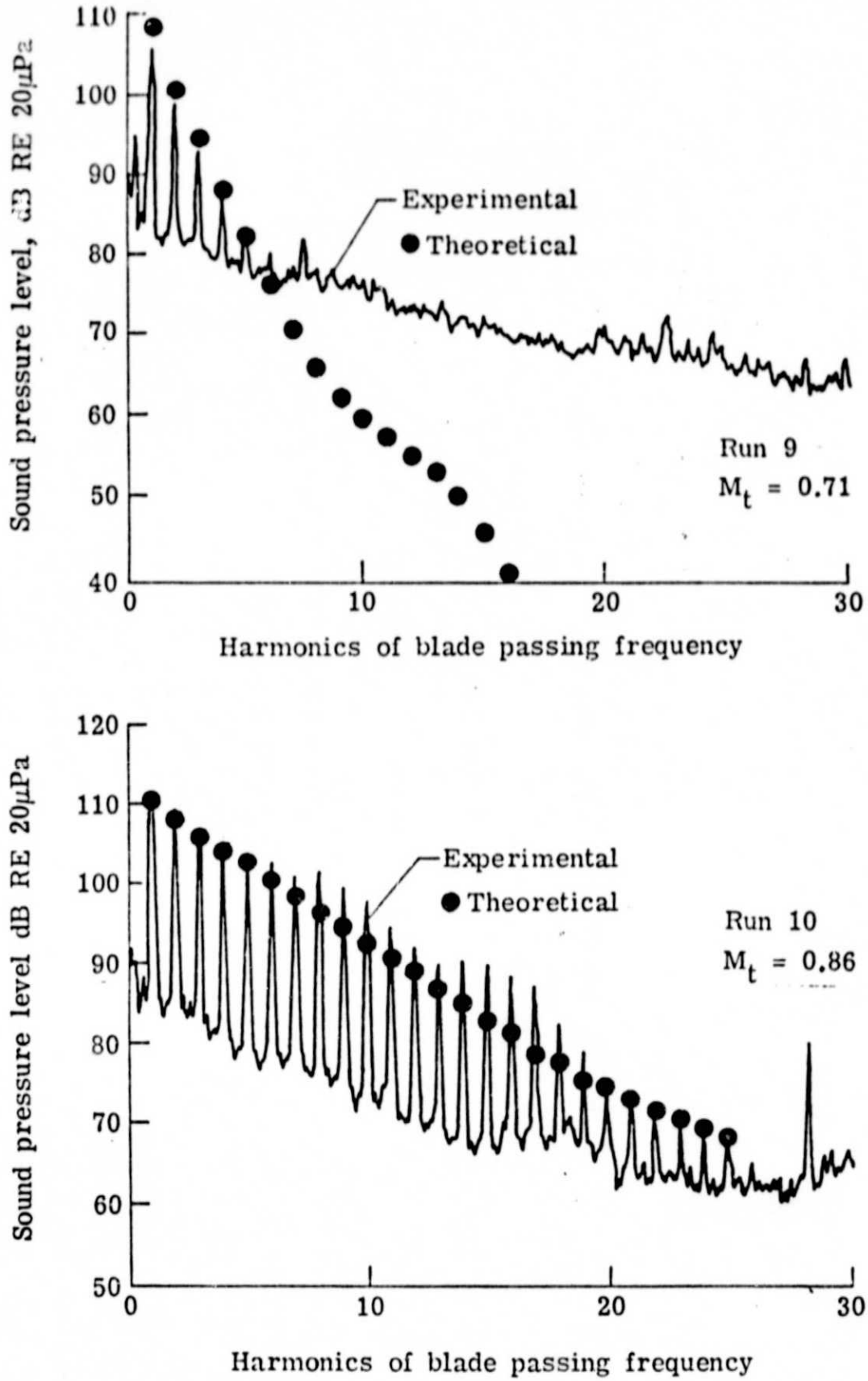

Figure 10.- Comparison of theoretical and measured acoustic spectra for two different helical tip speeds. In-plane microphone.

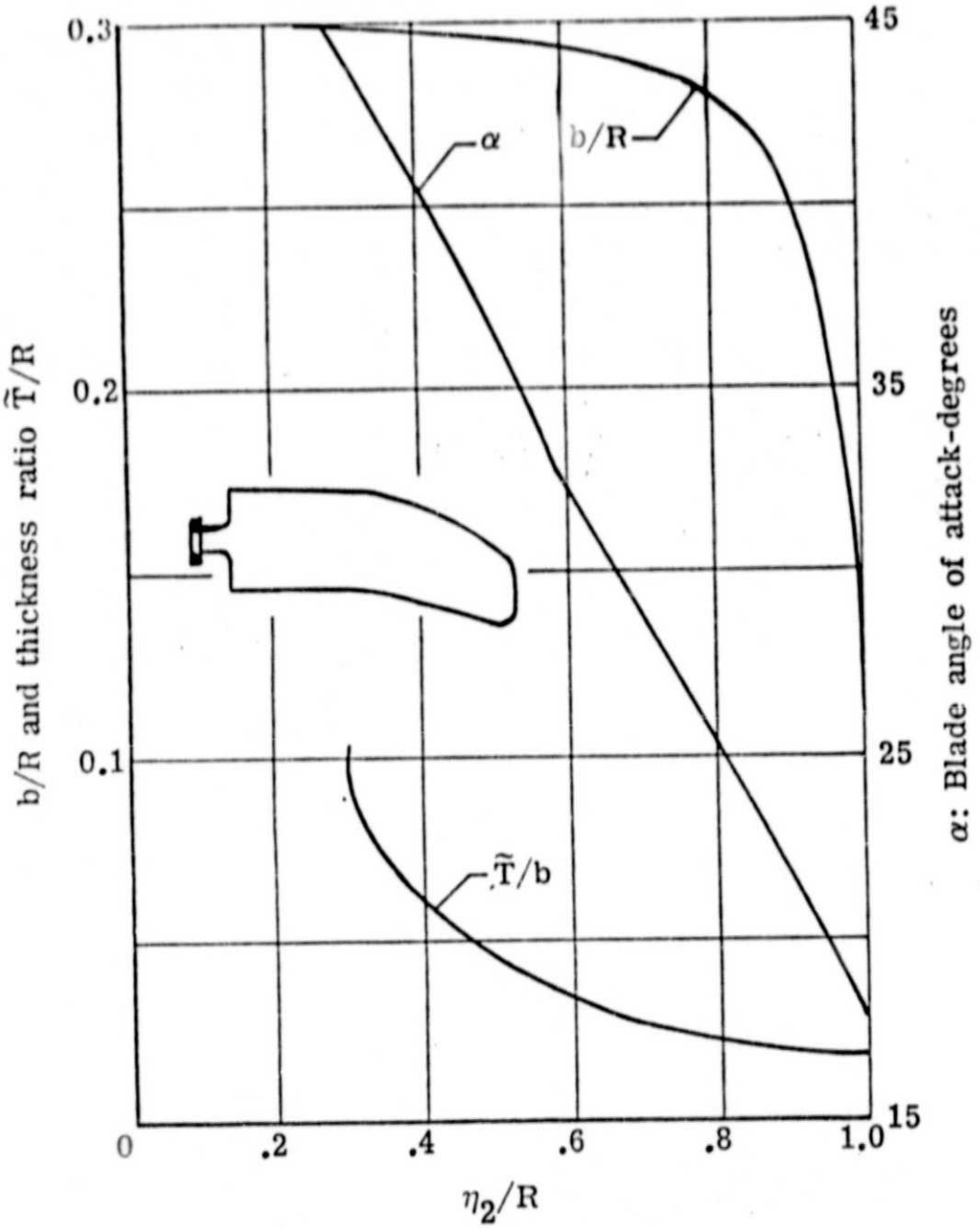

Figure 11.- Blade form curves and the planform for the advanced propeller. b = chord, T = maximum thickness of airfoil, R = blade radius, η_2 = distance from propeller center.

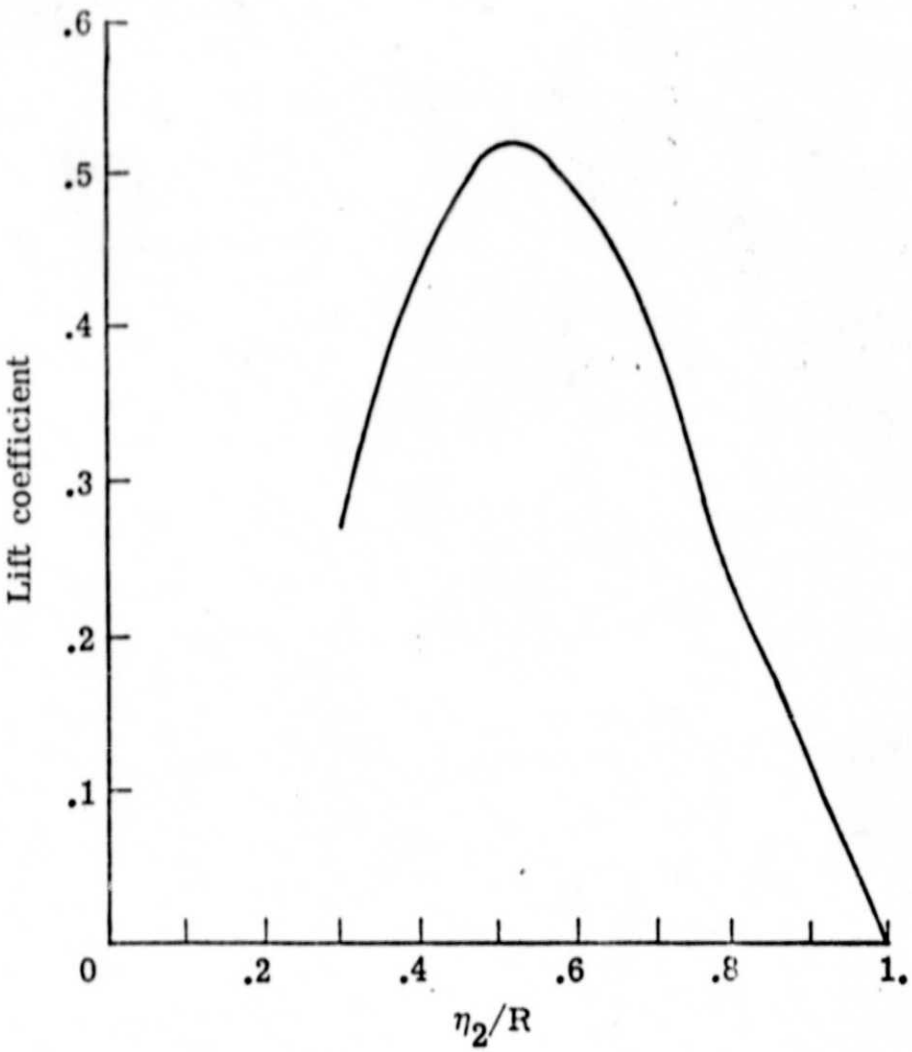

Figure 12.- Radial distribution of blade lift coefficient for the advanced propeller. η_2 = distance from propeller center.

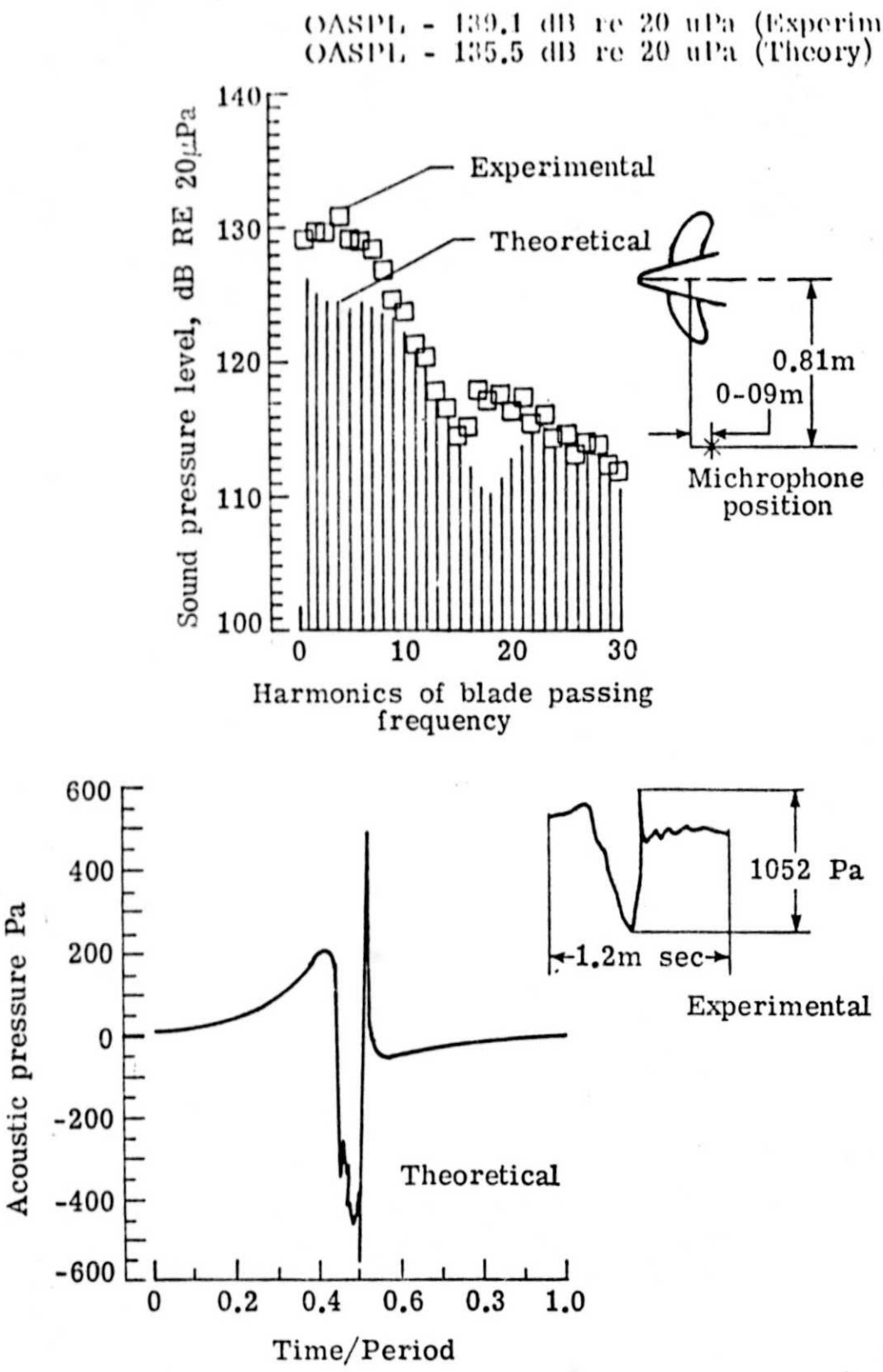

Figure 13.- Comparison of theoretical and experimental acoustic pressure signatures and spectra for the advanced propeller. Period = 2.667 msec, number of blades = 2.

OASPL = 135.2 dB RE 20 μPa (Experiment)
OASPL = 130.9 dB RE 20 μPa (Theory)

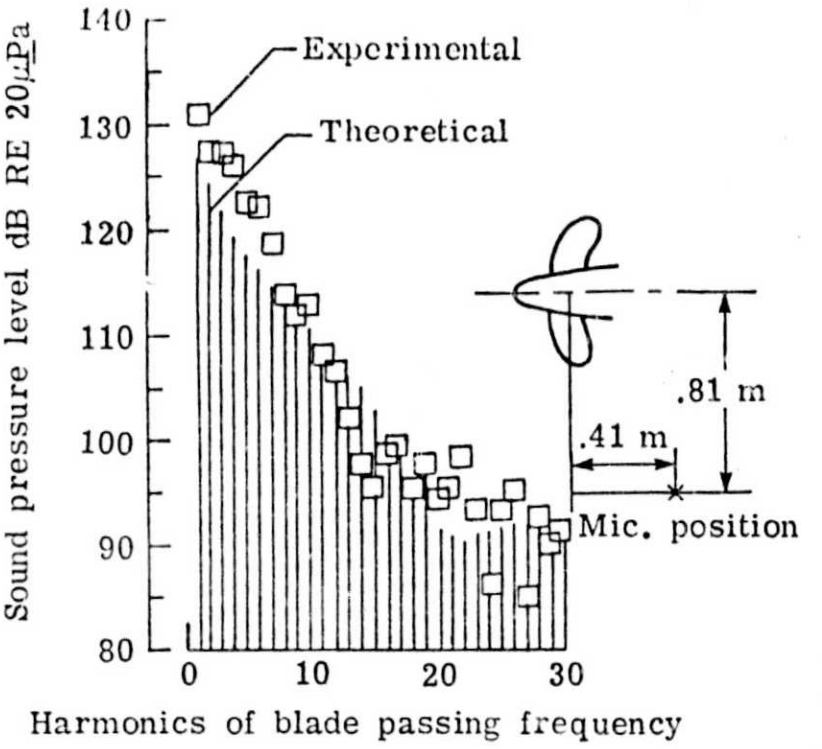

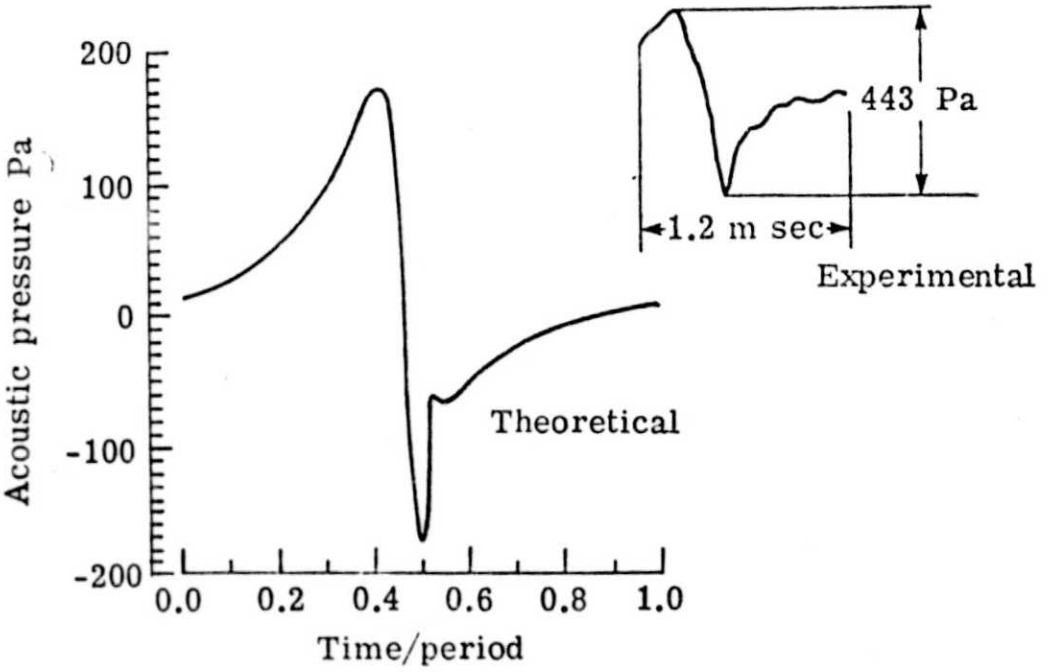

Figure 14.- Comparison of theoretical and experimental acoustic pressure signatures and spectra for the advanced propeller. Period = 2.667 msec, number of blades = 2.